Review of Overmodulation Control Techniques of Drive Inverters with Synchronous Space-Vector PWM

Valentin Oleschuk, Vladimir Ermuratskii, Irina Vasiliev
Institute of Power Engineering of Moldova
Chisinau, Republic of Moldova

***Abstract*—This manuscript presents short survey of basic techniques and algorithms of synchronous space-vector modulation for control of voltage source inverters of motor drives in the overmodulation control mode. These control regimes are characterized by specific control schemes which are differ from schemes of synchronous PWM for linear (undermodulation) control regimes of inverters. So, specialized overmodulation-focused schemes, techniques, and algorithms of synchronous PWM have been reviewed regarding some basic topologies of drive inverters: a) standard three-phase inverters; b) dual three-phase and six-phase systems; c) modular converters; d) triple-inverter-based systems, and e) five-phase inverters.**

Keywords—inverters; space vector pulse width modulation, motor drives, motion control, spectral analysis

I. INTRODUCTION

For drive inverters with low switching frequency, in order to eliminate undesirable subharmonics in spectra of its voltage and current, it is necessary to provide synchronization of voltage waveforms of inverters [1,2]. During the last decades, novel method of synchronous space-vector PWM for drive inverters has been elaborated based on new approach for determination of the pulse patterns [3,4]. It allows ensuring synchronization and symmetry of voltage waveforms of inverters both with integral and fractional ratio between the switching frequency and fundamental frequency of inverters. Also, special attention has been paid to analysis of overmodulation control modes of PWM inverters and drives [5-22]. Overmodulation regimes are ones of the most complicated control modes of converters and drives. So, this paper presents short review of methods and techniques of synchronous PWM, developed and modified for overmodulation control of some basic topologies of inverters.

II. BASICS OF OVERMODULATION CONTROL OF INVERTERS WITH SYNCHRONOUS SPACE-VECTOR MODULATION [7-9]

Methods of synchronous modulation, elaborated primarily for three-phase inverters [3,4], have been developed for linear control of the phase voltage of drive systems in the zone of overmodulation [7-22]. Fig. 1 presents basic structure of power circuits of three-phase inverter and its voltage vectors. Fig. 2 illustrates control and modulation parameters of inverter, and shows (inside the 90^0-interval) switching sequence of inverter, and the pole (Phases *a, b, c*) and line (V_{ab}) voltages of inverter with algorithms of discontinuous synchronous PWM [8].

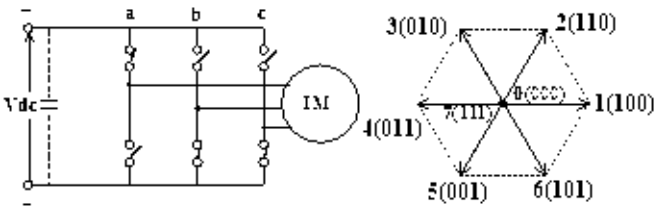

Fig. 1. Structure of three-phase voltage source inverter with induction motor IM, and its output voltage vectors [3].

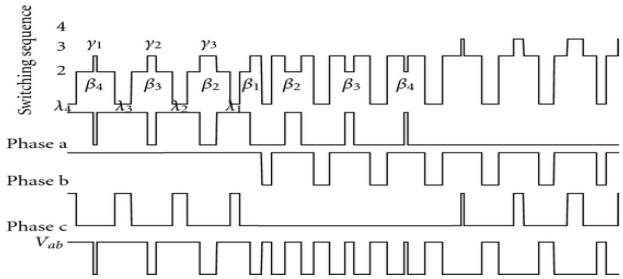

Fig. 2. Basic control/output signals of inverter with discontinuous PWM [3].

Typical control scheme for inverters with standard *V/F* control of drive system during overmodulation is based on two-stage strategy with two threshold frequencies $F_{ov1} = 45.35Hz$ (modulation index $m=0.907$ in this case) and $F_{ov2} = 47.6Hz$ ($m=0.952$) for systems with the maximum frequency F_m equal to *50Hz* [1,3-6]. So, control process consists from two stages in this zone. And special coefficients of overmodulation K_{ov1} (1) and K_{ov2} (2) are used in the modified control correlations of inverters with synchronous PWM, providing linear control of the fundamental voltage in this zone [8,10]:

$$K_{ov1} = 1- (F - F_{ov1})/(F_{ov2} - F_{ov1}) \quad (1)$$

$$K_{ov2} = 1- (F - F_{ov2})/(F_m - F_{ov2}) \quad (2)$$

During the first control stage of the overmodulation zone, between the frequencies F_{ov1} and F_{ov2}, a smooth linear increase of total active signals (β-parameters in Fig. 2) until the width of $\beta_1 = \tau$ (τ - switching cycle) is observed, with simultaneous smooth reduction of all notches λ until zero at the F_{ov2}. In the second zone, between F_{ov2} and F_m, here is a smooth decrease in the widths of all γ-parameters until zero at the six-step mode observed at F_m [8].

978-1-7281-6870-8/20/$31.00 ©2020 IEEE

Basic set of control functions of inverters with synchronous modulation for adjustment of drive systems during the whole control range (with overmodulation zone) includes (3)-(8) [8]:

$$\beta_j = \beta_1 \cos[(j-1.25)\tau K_{ov1}] \quad (3)$$

$$\gamma_j = \beta_{i-j+1}\{0.5-0.87\tan[(i-j-0.25)\tau]\}K_{ov2} \quad (4)$$

$$\beta_i = \beta'' = \beta_1 \cos[(i-1.25)\tau K_{ov1}]K_s \quad (5)$$

$$\gamma_1 = \beta''\{0.5-0.9\tan[(i-2.2)\tau+(\beta''+\lambda_{i-1})/2]\}K_s K_{ov2} \quad (6)$$

$$\lambda_j = \tau-(\beta_j+\beta_{j+1})/2 \quad (7)$$

$$\lambda_i = \lambda' = \left(\tau-\beta''\right)K_{ov1}K_s\,, \quad (8)$$

where $K_{ov1}=1$ until $F_{ov1}=0.907F_m$, $K_{ov2}=1$ until F_{ov2}, $\beta_1=1.1\tau m$ until $F_{ov1}=0.907F_m$ ($m = F/F_m$ – modulation index), and $\beta_1=\tau$ after F_{ov1}.

Figs. 3-4 present switching state sequence and voltage half-wave of inverter with discontinuous synchronous PWM with average switching frequency equal to *1.1kHz* [8,10].

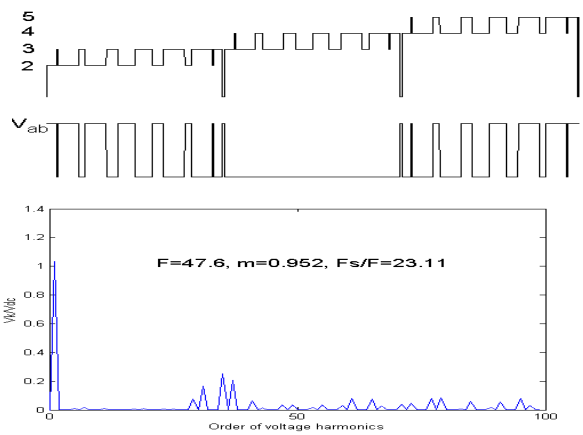

Fig. 3. Switching state sequence, line voltage of inverter and its spectrum for a half of period of the first overmodulation sub-zone (*F= 47.5Hz,m=0.95*) [8].

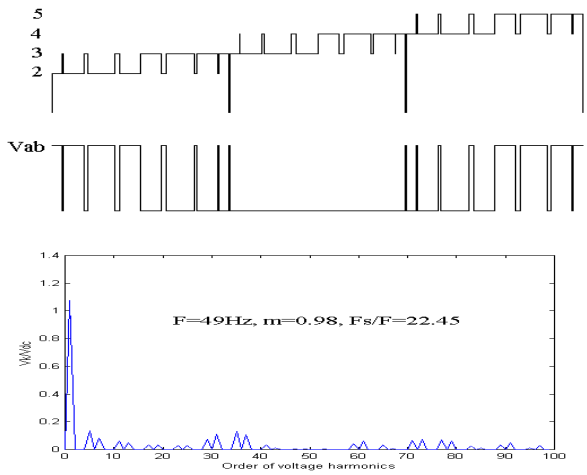

Fig. 4. Switching state sequences, line voltage of inverter and its spectrum at the second sub-zone of overmodulation range (*F= 49Hz, m=0.98*) [8].

III. Overmodulation Adjustment of Dual Three-Phase Inverters and Drives [11,12,14,16.17,20]

Dual three-phase (six-phase) induction motor drive fed by two three-phase voltage source inverters are between popular topologies of converters and drives [11,12,14]. Induction machine has in this case two sets of windings spatially shifted by 30 el. degrees with isolated neutral points (Fig. 5 [11]).

Figs. 6-13 present basic voltage and current waveforms (with its spectra) of dual three-phase drive controlled by algorithms of discontinuous synchronous PWM (DPWM) both in the first (Figs. 6-10) and the second (Figs. 11-14) parts of the zone of overmodulation. Average switching frequency of inverters is equal to *1kHz*. Fig. 8 and Fig. 13 present phase currents I_{as} of drive system with synchronous PWM with the 10kW dual-three-phase induction motor, and also the corresponding useful I_{sa} component of the phase current. Figs. 9, 10, and 14 show spectra of the corresponding currents [11].

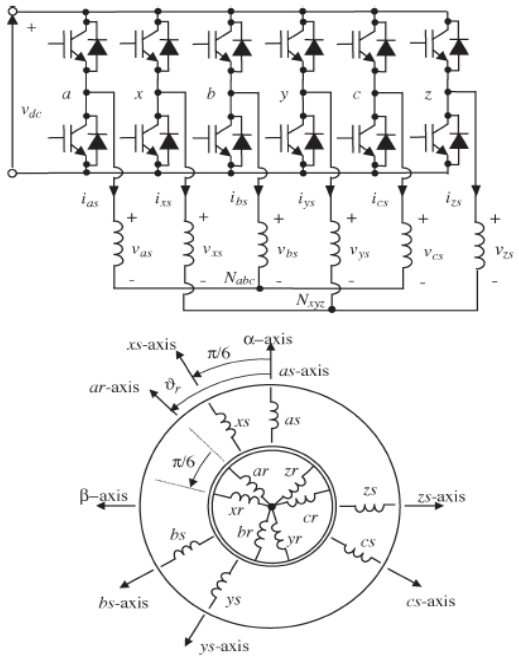

Fig. 5. Asymmetrical dual three-phase motor drive with single dc source [11].

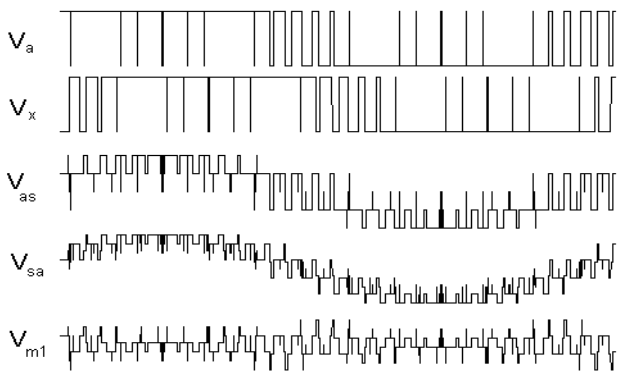

Fig. 6. Pole voltages V_a and V_x, phase voltage V_{as}, and useful (V_{sa}) and loss-producing (V_{m1}) components of the phase voltage for system with discontinuous synchronous PWM (DPWM) in overmodulation zone (*F=46.5Hz*) [11].

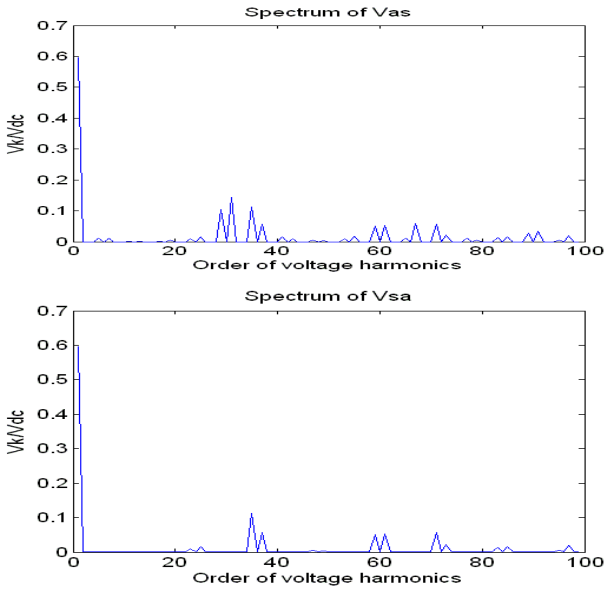

Fig. 7. Spectra of the V_{as} and V_{sa} voltages (DPWM, $F=46.5Hz$) [11].

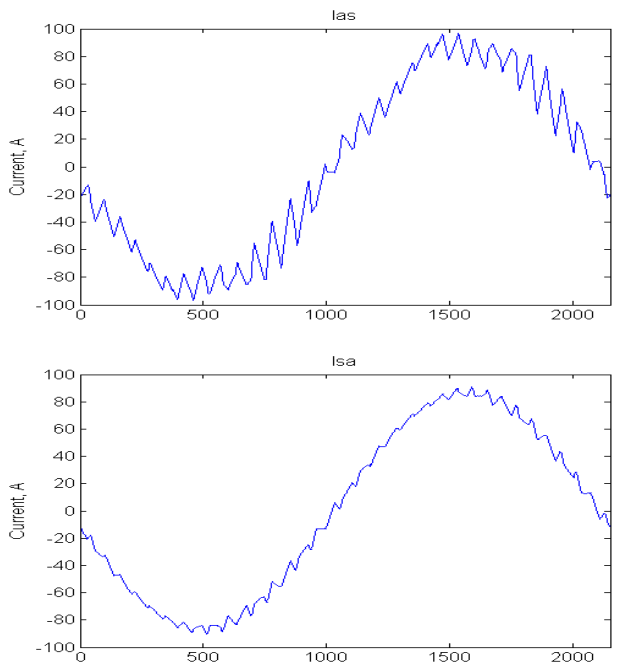

Fig. 8. Phase current I_{as}, and its I_{sa} component (DPWM, $F=46.5Hz$) [11].

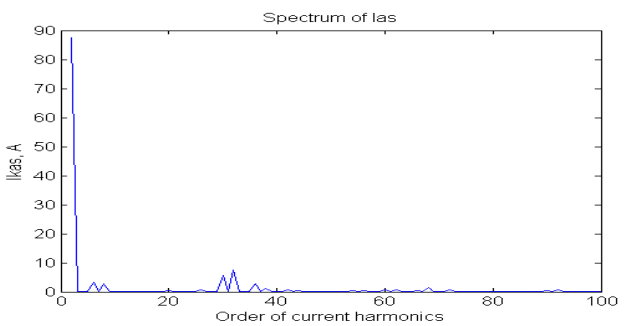

Fig. 9. Spectrum of the I_{as} for system with DPWM ($F=46.5Hz$) [11].

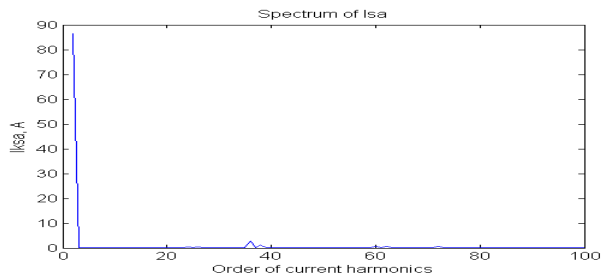

Fig. 10. Spectrum of the I_{sa} for system with DPWM ($F=46.5Hz$) [11].

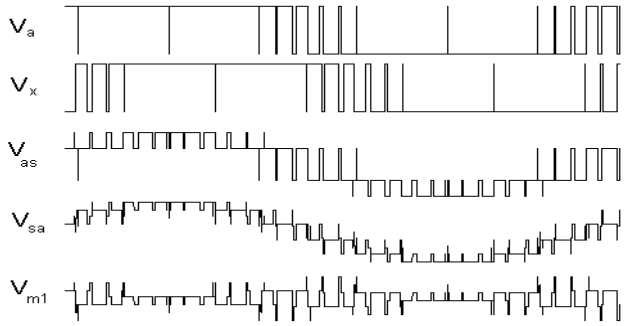

Fig. 11. Pole voltages V_a and V_x, phase voltage V_{as}, and useful (V_{sa}) and loss-producing (V_{m1}) components of the phase voltage for system with discontinuous synchronous PWM (DPWM) in overmodulation zone ($F=48.5Hz$) [11].

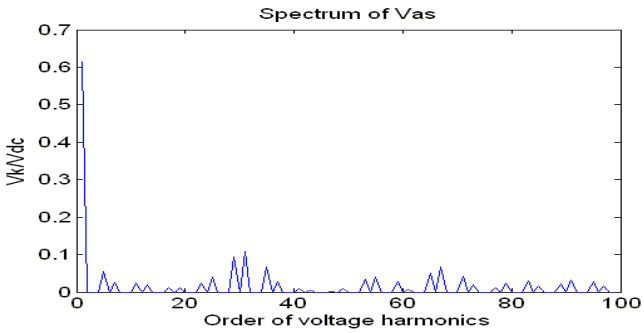

Fig. 12. Spectrum of the phase voltage V_{as} (DPWM, $F=48.5Hz$) [11].

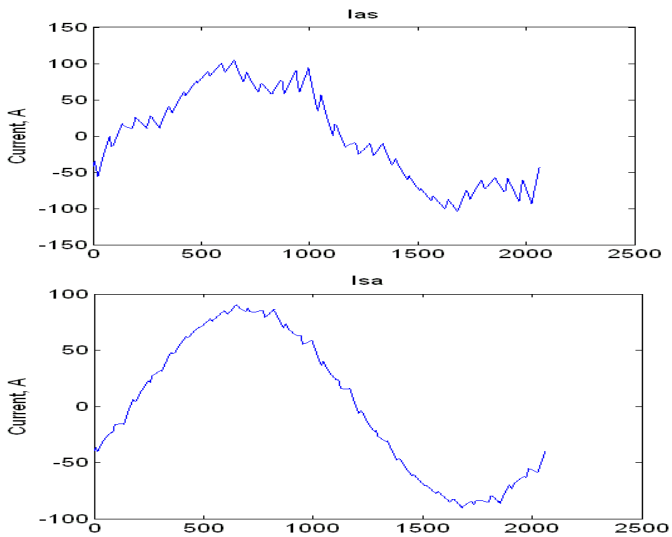

Fig. 13. Phase current I_{as}, and its I_{sa} component (DPWM, $F=48.5Hz$) [11].

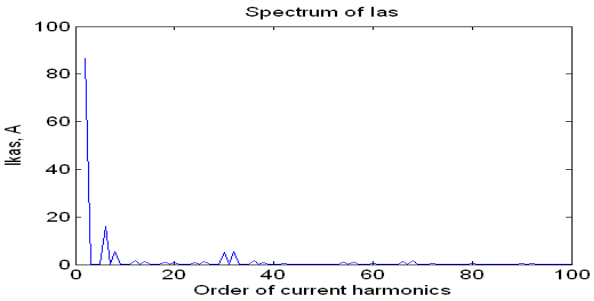

Fig. 14. Spectrum of the I_{as} current of the system (DPWM, *F=48.5Hz*) [11].

Fig. 15 presents results of calculation of Total Harmonic Distortion factor (THD) for the phase current I_{as} (averaged values of $THD = (1/I_{as1})\sqrt{\sum_{i=2}^{n} I_{asi}^2}$) of dual three-phase system with continuous (CPWM) and discontinuous (DPWM) versions of synchronous PWM. The average switching frequency of inverters is equal to *1kHz*, control mode corresponds here to standard scalar Volts/Hertz control. So, algorithms of synchronous DPWM assure better harmonic composition of the output voltage and current of system in comparison with the using of algorithms of CPWM.

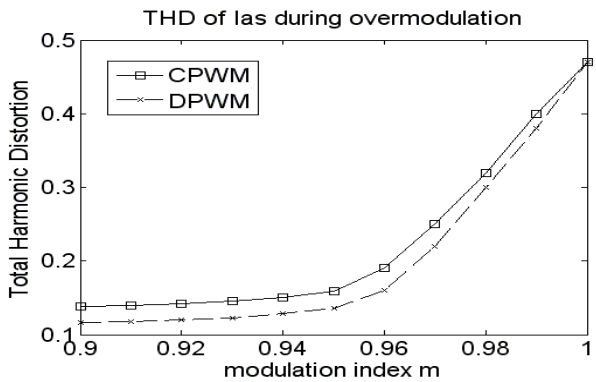

Fig. 15. Averaged *THD* factor of the I_{as} versus modulation index *m* [11].

IV. Flexible Overmodulation Control of Modular Converter [10]

Fig. 16 presents basic topology of modular converter consisting from three standard three-phase voltage source inverters along with a 0.33 p.u. output transformer and induction motor **M** as a load, which is especially useful for medium voltage application [10].

Fig. 17 and Fig. 18 show period of the line voltage of each inverter with synchronous discontinuous PWM and of the composed line voltage of modular converter (with an ideal transformer) with synchronous voltage control during the first (Fig. 15) and the second (Fig. 16) stages of the zone of overmodulation. Average switching frequency is equal to *700Hz*

Fig. 19 presents curves showing variation of the averaged Weighted Total Harmonic Distortion factor (*WTHD*) of the composed line voltage of cascaded converter as function of modulation index *m* during the zone of overmodulation, calculated for operating modes with both constant (mode 1) and variable (modes 2 and 3) phase shift between signals of three inverters. The presented results show, that variable phase shift of signals and output voltages of inverters assures improvement of value of *WTHD* factor for system operating at the second stage of the zone of overmodulation [10].

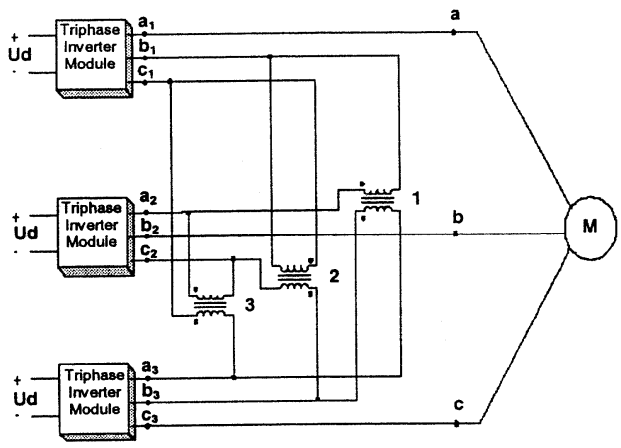

Fig. 16. Topology of modular converter consisting from three voltage source inverters, with an induction motor (**M**) as a load [10].

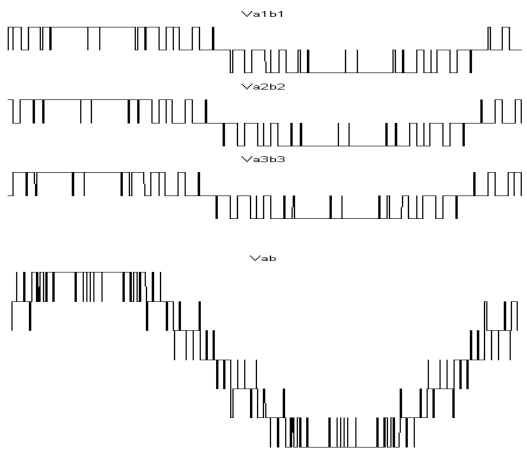

Fig. 17. Line voltages of modular converter (*F= 46Hz, m=0.92*) [10].

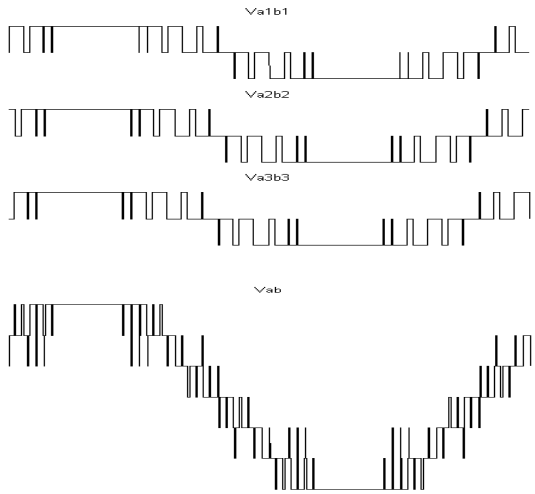

Fig. 18. Line voltages of modular converter (*F=48Hz, m=0.96*) [10].

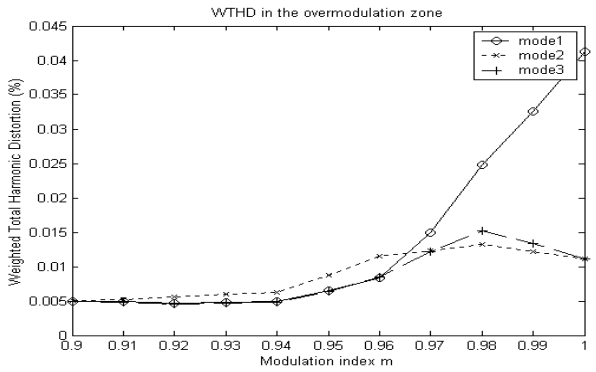

Fig. 19. *WTHD* of the composed line voltage of modular converter with constant (mode 1) and variable (modes 2-3) phase shift of signals of inverters [10].

V. Overmodulation Control of Triple Inverters of Transformer-Based Drive System [22]

Fig. 20 presents three-inverter-based drive system with double-delta configuration of inverter-side windings of power transformer [22]. For this topology of system, instantaneous value of winding voltage V_{w1} is determined during the whole adjustment range (including zone of overmodulation) as function of the pole voltages $V_{a10}-V_{c30}$ of three inverters:

$$V_{w1} = V_{a30} + (V_{a30}+V_{b30}+V_{c30})/3 - V_{b20} - (V_{a20}+V_{b20}+V_{c20})/3$$

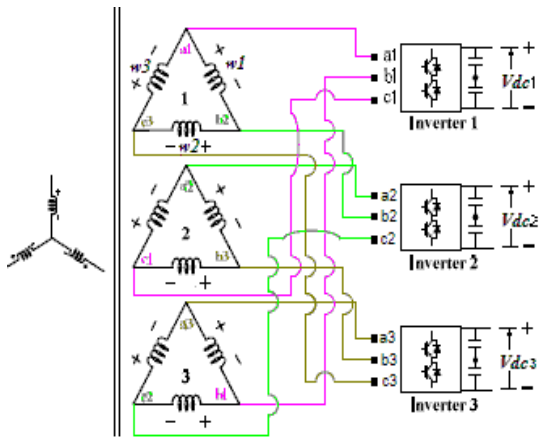

Fig. 20. Structure of power drive system based on three inverters with double-delta configuration of windings of power transformer [22].

Figs. 21-24 show simulation results of power installation based on three inverters ($V_{dc1}=V_{dc2}=V_{dc3}$), operating at the first part of the zone of overmodulation (Figs. 21-22), and at the second stage of overmodulation control (Figs. 23-24). Switching frequency of three inverters is equal to *1.05kHz* [22].

Fig. 25 presents diagram of Weighted Total Harmonic Distortion (*WTHD*) factor of the V_{a1b1} and V_{w1} voltages of drive installation with two basic sorts of synchronous discontinuous PWM $(WTHD = (1/V_{w1_1})(\sum_{k=2}^{1000}(V_{w1_k}/k)^2)^{0.5})$, and shows that *WTHD* factor of the V_{w1} voltage of the presented topology of ac drive system is better than *WTHD* factor of the line-to-line V_{a1b1} voltage of every inverter [22].

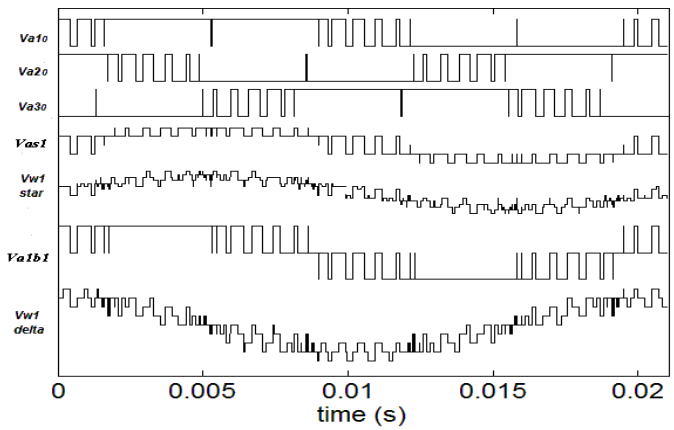

Fig. 21. Pole, phase, and line voltages V_{a10}, V_{b10}, V_{c10}, V_{as1}, V_{a1b1}, and winding voltages V_{w1star} and $V_{w1delta}$ of system with synchronous discontinuous PWM in the zone of overmodulation (DPWM30, $F=47.5Hz$, $F_s=1kHz$, $m=0.95$) [22].

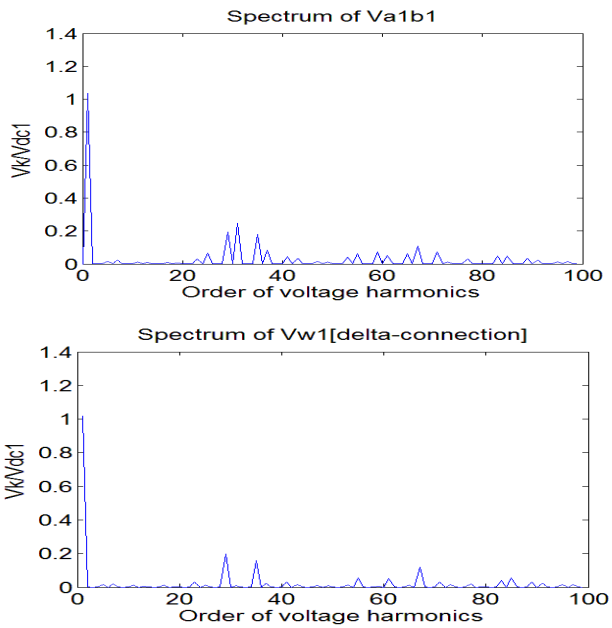

Fig. 22. Harmonic composition of the basic voltages of installation with discontinuous PWM (DPWM30, $F=47.5Hz$, $F_s=1kHz$, $F_s/F=21.1$, $m=0.95$) [22].

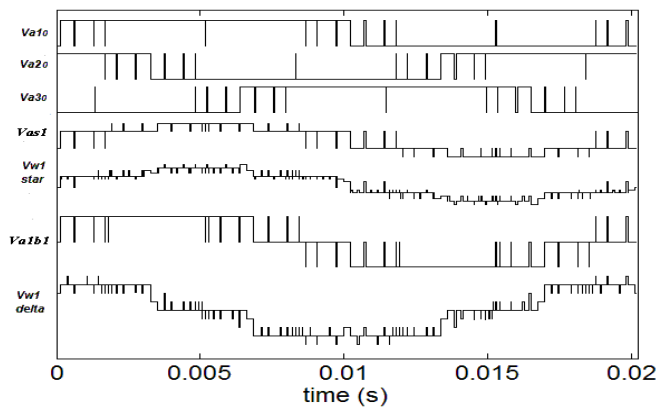

Fig. 23. Pole, phase, and line voltages V_{a10}, V_{b10}, V_{c10}, V_{as1}, V_{a1b1}, and winding voltages V_{w1star} and $V_{w1delta}$ of system with synchronous discontinuous PWM in the zone of overmodulation (DPWM30, $F=49.5Hz$, $F_s=1kHz$, $m=0.99$) [22].

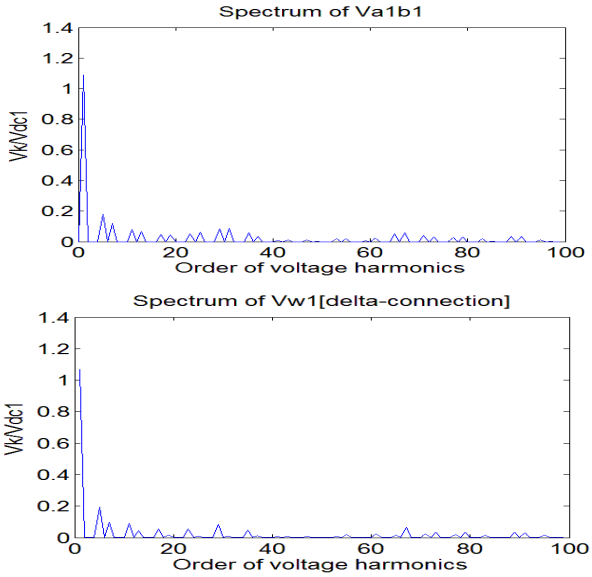

Fig. 24. Harmonic composition of the basic voltages of installation with discontinuous PWM (DPWM30, $F=49.5Hz$, $F_s=1kHz$, $F_s/F=21.1$, $m=0.99$) [22].

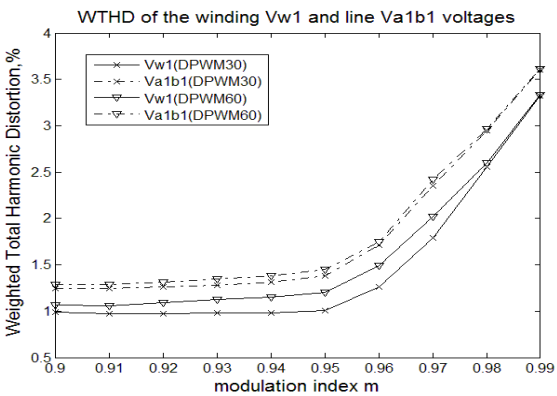

Fig. 25. *WTHD* factor of basic voltages of power installation as function of coefficient of modulation m ($F_s=1kHz$) [22].

Results of simulation of system, presented in Figs. 21–24, show, that for the all analyzed control modes both line voltages and winding voltages have quarter-wave symmetry and are characterized by the absence in its voltage spectra of even harmonics and subharmonics.

VI. Synchronous Overmodulation Control of Five-Phase Inverters [15,18,19,21]

Novel strategy of synchronous control of inverters in the zone of overmodulation, with specific peculiarities of the used scheme of synchronous multi-zone PWM, has been applied for control of five-phase inverters [15,18,19,21]. In accordance with this PWM strategy, developed and disseminated for five-phase systems, the proposed three-stage control process insures smooth transition to the ten-step control mode at the maximum fundamental frequency of five-phase installation.

Structure of basic power circuits of five-phase inverter with neutral point n is illustrated by Fig. 26 [18]. For this system, mutual phase shift between voltages of phases a, b, c, d and e is equal to 72 el. grad. Fig. 27 presents diagram of voltage space-vectors of five-phase system consisting from ten large (**1, 2, 3, 4, 5, 6, 7, 8, 9, 10**) and ten medium (**1', 2', 3', 4', 5', 6', 7', 8', 9', 10'**) voltage space-vectors designated (by five-digit numbers) in accordance with standard designation [19].

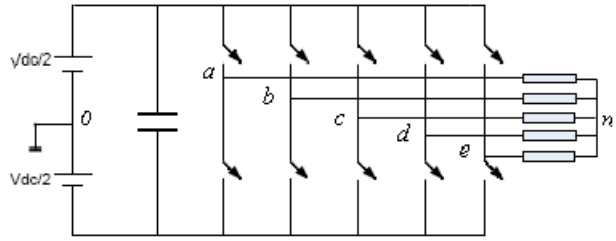

Fig. 26. Structure of five-phase inverter system [18].

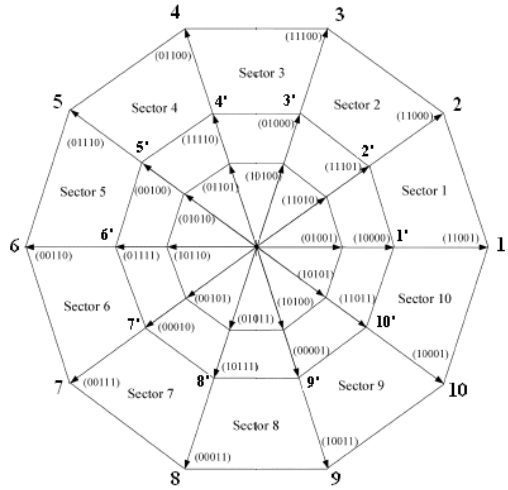

Fig. 27. Voltage spece-vectors of five-phase installation [19].

A. *The First Stage of Synchronous Overmodulation Control*

In order to obtain linearity of the fundamental voltage/ fundamental frequency (*Volts/Hertz*) characteristic of five-phase system with standard scalar control mode during the whole control diapason, scalable coefficient equal to $0.64/0.53=1.20$ should be included in the corresponding correlations providing determination of widths (of duration) of the corresponding active switching states of five-phase inverter with synchronous PWM [19].

So, the first inverter modulation index m_{ov1}, characterizing the beginning of operation of inverter in the zone of overmodulation, can be calculated as

$$m_{ov1} = 0.53/0.64 = 0.83 \quad (9)$$

In particular, if the maximum fundamental frequency $F_{ten\text{-}step}=50Hz$, the threshold fundamental frequency F_{ov1}, which characterizes the beginning of the zone of overmodulation of five-phase inverter with scalar control, is equal to $F_{ov1} = m_{ov1} F_{ten\text{-}step}=41.5Hz$.

The second threshold modulation index in accordance with (9) is determined as [19]

$$m_{ov2} = 0.615/0.64 = 0.97 \quad (10)$$

The second threshold fundamental frequency F_{ov2}, which characterizes the upper limit of the first control stage in the zone of overmodulation of five-phase inverter with scalar control ($F_{ten\text{-}step}=50Hz$), is equal to $F_{ov2} = m_{ov2}F_{ten\text{-}step}=48.34Hz$.

To allow synchronous character of PWM processes during control of five-phase system in the first part of overmodulation range, special coefficient K_{ov1} (11), connecting modulation index m of inverter with two threshold indices m_{ov1} and m_{ov2}, is included in basic control correlations in this sub-zone [19]:

$$K_{ov1} = 1- (m - m_{ov1})/(m_{ov2} - m_{ov1}) \quad (11)$$

So, during the first control stage of the overmodulation zone, between fundamental frequencies F_{ov1} and F_{ov2}, a smooth linear decrease of widths of the δ_k' and δ_k'' active signals [19] is observed in accordance with (12):

$$\delta_k'+\delta_k''= 0.382\beta_{i-k+1}K_{ov1} \quad (12)$$

Fig. 28 ($F=43Hz$, $m=0.86$) illustrates synchronous voltage control of five-phase inverter during the first control stage of the overmodulation zone [19]. The presented in Fig. 28 curves of the output voltage of inverter have quarter-wave symmetry, and its spectra are without undesirable subharmonics.

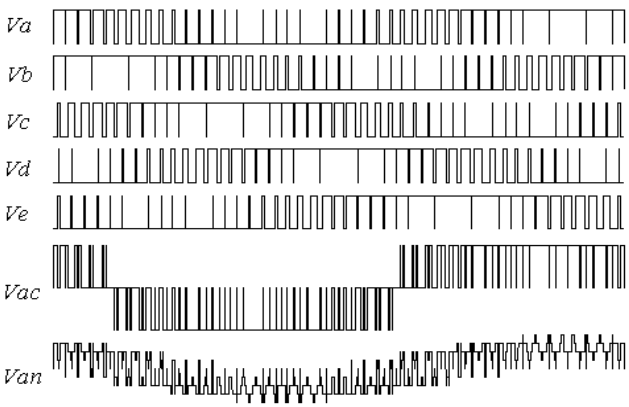

Fig. 28. Pole voltages $V_a - V_c$, line and phase voltages V_{ac} and V_{an}, of five-phase system at the first part of overmodulation zone ($F=43Hz$, $m=0.86$) [19].

B. The Second Stage of Synchronous Overmodulation Control

During the second stage, realization of control functions (13)-(15) provides smooth synchronous decrease of durations of all notches (13) together with simultaneous increasing of widths of the total active β–signals (14) until the maximum duration, equal to the duration of sub-cycle τ [19].

$$\lambda_j = [\tau - (\beta_j + \beta_{j+1})/2]K_{ov2} \quad (13)$$

$$\beta_j = \tau\cos[(j-1)\tau K_{ov2}] \quad (14)$$

$$K_{ov2} = 1- (m - m_{ov2})/(m_{ov3} - m_{ov2}) \quad (15)$$

To illustrate modulation process in system during the second part of overmodulation zone, Fig. 29 presents basic voltages of five-phase inverter ($F=48.75Hz$, $m=0.975$). The switching frequency is equal to $3kHz$ in this case [19].

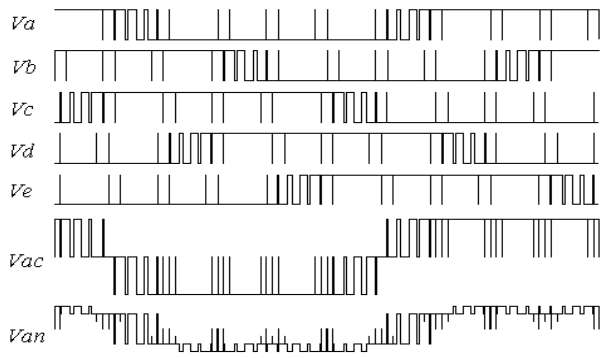

Fig. 29. Basic voltages of five-phase inverter at the second part of the overmodulation zone ($F = 48.75$ Hz, $m = 0.975$) [19].

C. The Third Stage of Synchronous Overmodulation Control

To insure smooth transition of five-phase system to the ten-step control mode at the maximum fundamental frequency of inverter ($m=1$ in this case), the third specific coefficient of overmodulation K_{ov3} (16) should be included in equations (17)-(18), and its realization assures providing smooth decrease until zero of the widths of the γ-signals in this control sub-zone:

$$K_{ov3}=1-(m-m_{ov3})/(m_{ten\text{-}step}-m_{ov3})=1-(m-m_{ov3})/(1-m_{ov3}) \quad (16)$$

$$\gamma_j = \beta_{i-j+1}\{0.5 - 0.809\tan[(i-j)\tau]\}K_{ov3} \quad (17)$$

$$\gamma_1 = 5\beta''(\lambda' + \beta'')FK_sK_{ov3} \quad (18)$$

Fig. 30 presents basic voltage waveforms of five-phase inverter operating in the third part of the zone of overmodulation ($F = 49.6$ Hz, $m = 0.992$). The switching frequency is equal to $3kHz$. Fig. 31 presents basic voltage waveforms of five-phase inverter at the maximum fundamental frequency $F_{ten-step}=50Hz$, at the ten-step operation mode ($m=1$).

The described scheme of synchronous space-vector PWM of five-phase system with scalar V/F control insures both good utilization of dc-voltage and process of linear control of the fundamental voltage during the whole control range. Fig. 32 shows this linear variation of the first harmonic of the fundamental voltage of inverter versus modulation index m.

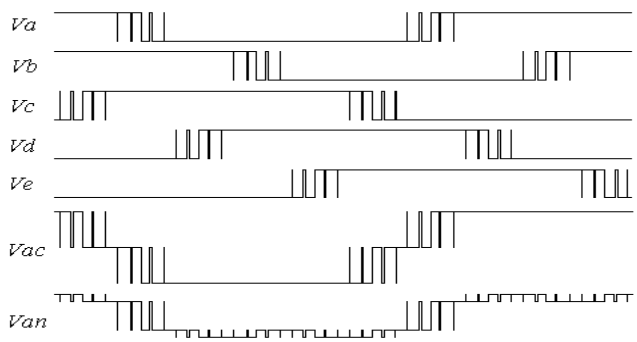

Fig. 30. Basic voltages of five-phase inverter at the third part of the overmodulation zone ($F=49.6Hz$, $m=0.992$) [19].

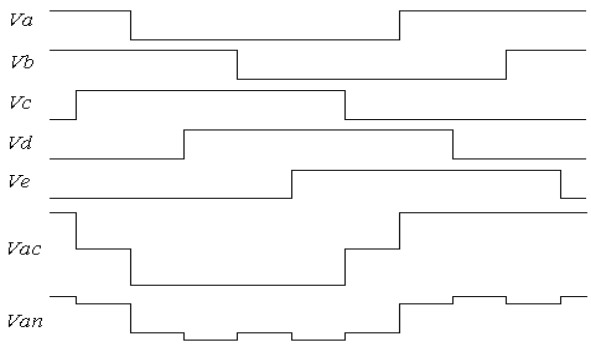

Fig. 31. Basic voltages of five-phase inverter at the ten-step control regime (*F=50Hz, m=1*) [19].

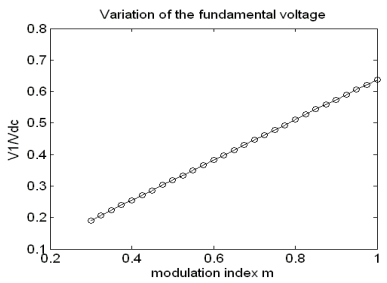

Fig. 32. Fundamental voltage versus coefficient of modulation m of five-phase system with synchronous multi-zone modulation [19].

VII. Conclusions

Overmodulation modes are ones of the most complicated and sophisticated control regimes of power converters. Specialized overmodulation-focused schemes and algorithms of synchronous multi-zone space-vector modulation, reviewed in the paper, assure both linear control of the fundamental voltage of drive inverters and symmetry of waveforms of the output voltage of drive inverters in this specific control zone.

It has been shown in the presented review, that two-stage control scheme in the zone of overmodulation is the most suitable for adjustment of standard three-phase inverters with synchronous PWM, of dual three-phase and six-phase inverter systems, of modular converters, of transformer-based triple-inverter systems. And for five-phase systems, due to its specific peculiarities, rational control scheme in the overmodulation range consists from three stages.

Overmodulation-oriented techniques and algorithms of synchronous PWM insure quarter-wave or half-wave symmetry of the output voltage of inverters, spectra of which do not contain even harmonics and subharmonics, which is especially important for the medium-power and high-power systems with low switching frequency of inverters.

References

[1] J. Holtz, “Pulsewidth modulation for electronic power conversion,” IEEE Proceedings, vol. 82, no. 8, pp. 1194-1213, 1994.

[2] N. Mohan, T.M. Undeland, and W.P. Robbins, Power Electronics, 3rd ed., John Wiley & Sons, 2005.

[3] V. Oleschuk and F. Blaabjerg, “Direct synchronized PWM techniques with linear control functions for adjustable speed drives,” Proc. of IEEE Appl. Power Electr. Conf. (APEC’02), 2002, pp. 76-82.

[4] F. Blaabjerg, V. Oleschuk, and F. Lungeanu, “Synchronization of output voltage waveforms in three-phase inverters for induction motor drives,” Proc. of IEEE-IEEJ Power Conversion Conf. (PCC’2002), 2002, pp. 528-533.

[5] S.K. Mondal, B.K. Bose, V. Oleschuk, and J. Pinto, "Space vector pulse width modulation in three-level inverter extending operation into overmodulation region", IEEE Trans. on Power Electr., vol. 18, no. 2, pp.604-611, 2003.

[6] C. Wang, B.K. Bose, V. Oleschuk, S. Mondal, and J. Pinto, “Neural-network-based space-vector PWM of a three-level inverter covering overmodulation region”, Proc. of IEEE Ind. Electronics Conf. (IECON'03), 2003, pp.1-6.

[7] V. Oleschuk, B.K. Bose, and Zhe Chen, “Synchronized overmodulation techniques for neutral-clamped inverters”, Proc. of IEEE Power Electronics Specialists Conf. (PESC’03), 2003, pp.41-46.

[8] V. Oleschuk, V. Ermuratski, and E.M. Chekhet, “Drive converters with synchronized PWM during overmodulation”, Proc. of IEEE Int’l Symp. on Ind. Electronics (ISIE’2004), 2004, pp.1339-1344.

[9] V. Oleschuk, V. Ermuratski, A. Sizov, and E. Yaroshenko, “Synchronous voltage control in the overmodulation zone of drive inverters”, Technical Electrodynamics, no. 1, pp. 22-29, 2004.

[10] V. Oleschuk, V. Ermuratski, and A.M. Stankovic, “Modular converters with synchronized control in the overmodulation zone”, Proc. of IEEE Power Electronics Specialists Conf. (PESC’2005), 2005, pp. 1227-1233.

[11] V. Oleschuk, R. Bojoi, F. Profumo, and A.M. Stankovic, “Operation of six-phase drives with synchronized PWM in the overmodulation region,” Proc. of IEEE Int’l Conf. on Ind. Technology (ICIT’2006), 2006, pp. 1293-1300.

[12] V. Oleschuk, G. Griva, F. Profumo, and A. Tenconi, “Synchronized PWM control of symmetrical six-phase drives,” Proc. of IEEE Int’l Conf. on Power Electronics (ICPE’2007), 2007, pp. 147-152.

[13] V. Oleschuk, V. Ermuratski, and E. Yaroshenko, “Open-end winding motor drive with synchronous PWM in the overmodulation region”, Proc. of Development and Application Systems Conf. (DAS’2008), 2008, pp. 79-84.

[14] V. Oleschuk, R. Prudeak, A. Sizov, and E. Yaroshenko, “Asymmetrical six-phase drive with synchronized PWM during overmodulation,” Technical Electrodynamics, no. 5, pp. 34-37, 2008.

[15] V. Oleschuk, F. Profumo, A. Tenconi, and E. Yaroshenko, “Five-phase inverters with synchronized PWM,” Proc. of IEEE EUROCON’2007 Conf., 2007, pp. 1872-1858.

[16] V. Oleschuk, R. Bojoi, G. Griva, and F. Profumo, “Flexible synchronized control of dual inverter-fed traction drive during overmodulation”, Proc. of IEEE Advanced Motion Control Workshop (AMC’2008), 2008, pp. 704-709.

[17] G. Griva, V. Oleschuk, and F. Profumo, “Synchronized overmodulation techniques for symmetrical dual three-phase converters,” Proc. of IEEE Int’l Symp. on Power Electronics, Electrical Drives, Automation and Motion (SPEEDAM’2008), 2008, pp. 981-986.

[18] V. Oleschuk, G. Griva, R. Prudeak, and A. Sizov, “Three-stage synchronous overmodulation control of five-phase inverter,” Problems of the Regional Energetics, vol. 6, no. 1, pp. 53-64, 2010.

[19] G. Graditi, G. Griva, and V. Oleschuk, “Overmodulation control of five-phase inverters with full dc-bus voltage utilization,” Proc. of IEEE Symp. on Power Electron., Electrical Drives, Automation and Motion (SPEEDAM’2010), 2010, pp. 838-843.

[20] V. Oleschuk and A. Sizov, “Synchronous PWM control of symmetrical dual three-phase drive in the overmodulation zone,” Problems of the Regional Energetics, vol. 9, no. 1, pp. 19-27, 2013.

[21] V. Oleschuk and F. Barrero, “Standard and non-standard approaches for voltage synchronization of drive inverters with space-vector PWM: A survey,” International Review of Electrical Engineering, vol. 9, no. 4, pp. 688-707, 2014.

[22] V. Oleschuk and V. Ermuratskii, “Multi-inverter drive with symmetrical multilevel winding voltage of transformer during overmodulation,” Proc. of IEEE Int’l Symp. on Electrical and Electronic Engineering (ISEEE’2017), 2017, 5 p.